

This paper is published as part of a *Dalton Transactions* themed issue on:

Metal Anticancer Compounds

Guest Editor Peter Sadler

University of Warwick, UK

Published in [issue 48, 2009](#) of *Dalton Transactions*



Image reproduced with permission of Chi-Ming Che

Articles published in this issue include:

PERSPECTIVES:

[Non-traditional platinum compounds for improved accumulation, oral bioavailability, and tumor targeting](#)

Katherine S. Lovejoy and Stephen J. Lippard, *Dalton Trans.*, 2009, DOI: 10.1039/b913896j

[Metal complexes as photochemical nitric oxide precursors: Potential applications in the treatment of tumors](#)

Alexis D. Ostrowski and Peter C. Ford, *Dalton Trans.*, 2009, DOI: 10.1039/b912898k

[Novel and emerging approaches for the delivery of metallo-drugs](#)

Carlos Sanchez-Cano and Michael J. Hannon, *Dalton Trans.*, 2009, DOI: 10.1039/b912708a

HOT ARTICLE:

[Iron\(III\) complexes of fluorescent hydroxamate ligands: preparation, properties, and cellular processing](#)

Antonia J. Clarke, Natsuho Yamamoto, Paul Jensen and Trevor W. Hambley, *Dalton Trans.*, 2009, DOI: 10.1039/b914368h

Visit the *Dalton Transactions* website for more cutting-edge inorganic and bioinorganic research
www.rsc.org/dalton

Naphthalimide gold(I) phosphine complexes as anticancer metallodrugs†

Christoph P. Bagowski,^a Ya You,^b Heike Scheffler,^b Danielle H. Vlecken,^a Daan J. Schmitz^a and Ingo Ott^{*c}

Received 24th June 2009, Accepted 7th October 2009

First published as an Advance Article on the web 28th October 2009

DOI: 10.1039/b912378d

Gold(I) phosphine complexes exhibit promising properties for anticancer drug development. Here we report on a series of gold(I) phosphine complexes containing a naphthalimide ligand. Strong antiproliferative effects were observed in MCF-7 breast cancer cells as well as in HT-29 colon carcinoma cells. The cellular and nuclear gold levels were increased compared to analogues, in which the naphthalimide ligand was replaced by a chloro ligand. Compound **4a** was selected for more detailed biochemical and biological studies, which revealed solvent dependent fluorescence emission, uptake of the compound into the organelles of tumor cells as well as antiangiogenic effects concerning angiogenesis and tumor-induced angiogenesis *in vivo*. Antiangiogenic properties of **4a** were observed in two different zebrafish angiogenesis models, including a tumor-cell induced neovascularization assay.

Introduction

Platinum complexes have been playing an important role in modern tumor chemotherapy for approximately three decades but major problems, *e.g.* the occurrence of severe side effects, the development of drug resistance or the limited applicability to many widespread malignancies, have not yet been resolved.¹

Current strategies to overcome these obstacles focus on the optimisation of the clinical application of the existing platinum drugs, *e.g.* the use of platinum compounds for breast cancer therapy,² or the development of novel transition metal complexes containing improved organic ligands.^{3–7}

An increasing number of reports describe gold complexes with properties relevant for the design of novel anticancer therapeutics. Many derivatives trigger significant antiproliferative effects accompanied by the induction of apoptosis and antimitochondrial effects. The enzyme thioredoxin reductase (TrxR), which is involved in various tumor related biochemical pathways, has been identified as probably being the most relevant molecular target for gold complexes,^{8–10} and promising antiproliferative activity has been reported for a variety of different gold compounds including N-heterocyclic carbene species^{11,12} and gold(III) complexes.^{13–17}

Recently, we described a novel antiproliferative gold(I) phosphine compound containing a naphthalimide ligand (Au-Naphth-1, Fig. 1).¹⁸ The design of this compound is based on observations on the lead compound auranofin, which had indicated that the thiol-carbohydrate moiety of this metallodrug was exchanged during cell experiments.^{19,20} Replacement of this ligand with

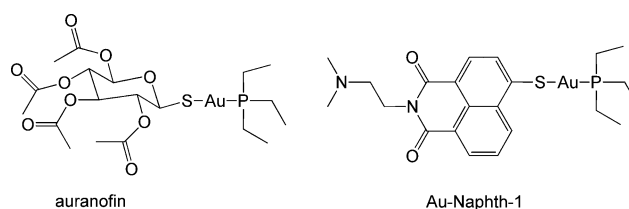


Fig. 1 Gold(I) phosphine complexes.

ligands displaying pharmacological activity themselves could lead to new agents with the capability of addressing multiple tumor-relevant targets. Accordingly, naphthalimides were chosen as a suitable class of bioactive ligands with significant cell growth inhibiting properties.^{21–24}

In fact, it was observed that the organic ligand in Au-Naphth-1 was responsible for an accumulation of gold in the nuclei and the triggering of antiangiogenic effects in developing zebrafish embryos. Furthermore, the inhibition of thioredoxin reductase by Au-Naphth-1 could be related to the presence of the gold phosphine moiety.¹⁸

In another recent study we evaluated the biodistribution profile of a series of chloro gold(I) phosphine derivatives.²⁵ These studies showed a rather low uptake of gold in the nuclei of tumor cells for these kind of gold phosphine complexes and indicated that larger, more lipophilic ligands at the phosphor center are able to slightly increase the overall cellular uptake and biodistribution of gold into the nuclei.

In continuation of these studies we prepared a series of naphthalimide gold(I) phosphine complexes and evaluated their cytotoxic properties and biodistribution. Compounds with different alkyl and aryl substituents on the phosphor were prepared in order to evaluate the influence of these substituents on the bioactivity and to shed more light on the general biological functions of gold phosphine complexes with naphthalimide ligands. One compound was selected for further studies concerning fluorescence monitoring and antiangiogenic properties (angiogenesis and tumor-induced angiogenesis).

^aDepartment of Integrative Zoology, Institute of Biology, University of Leiden, 2333 AL Leiden, The Netherlands

^bInstitute of Pharmacy, Freie Universität Berlin, Königin-Luise-Str 2+4, 14195 Berlin, Germany

^cInstitute of Pharmaceutical Chemistry, Technische Universität Braunschweig, Beethovenstr. 55, 38106 Braunschweig, Germany. E-mail: ingo.ott@tu-bs.de

† Electronic supplementary information (ESI) available: Studies on the inhibition of angiogenesis in zebrafish embryos and reduction of tumor cell-induced neovascularization in a zebrafish/tumor xenograft angiogenesis assay by a non-metal naphthalimide derivative. See DOI: 10.1039/b912378d

Results and discussion

Synthesis

The target compounds **1a–4a** were prepared by a convenient recently reported procedure starting from 4-mercaptanaphthalic anhydride (Fig. 2), and finally isolated by column chromatography.¹⁸ The structures were confirmed by ¹H-NMR-spectroscopy, EI-MS spectroscopy and elemental analyses.

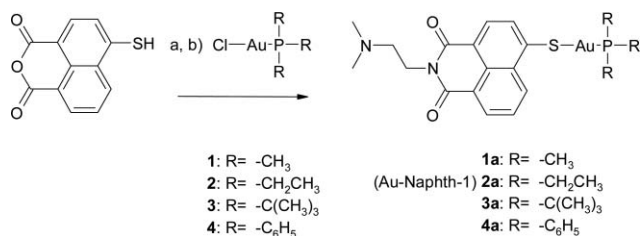


Fig. 2 Synthesis of **1a–4a**, (a) 2-(dimethylamino)ethylamine, EtOH, reflux heating, 6 h; (b) CH₂Cl₂, room temperature, 5 h.

Cell growth inhibitory effects, uptake into tumor cells and into nuclei

The cell growth inhibitory effects of the naphthalimide gold(i) phosphine target complexes **1a–4a** were evaluated in comparison to the respective chloro analogues **1–4** in HT-29 colon carcinoma and MCF-7 breast cancer cells (see Table 1). Concerning the trimethyl-, triethyl- and tri-*tert*-butyl analogues, the naphthalimide containing complexes were approximately twice as active as the chloro complexes whereas the activities of Cl-Au-P(Ph)₃ (**4**) and Naphth-Au-P(Ph)₃ (**4a**) did not significantly differ. IC₅₀ values for **1a** to **4a** were in the range of 1.1 to 3.7 μM, which is within the range of the gold(i) phosphine lead compound auranofin (IC₅₀ values of 2.6 μM in HT-29 cells²⁶ and 1.1 μM in MCF-7 cells²⁷), the platinum anticancer drug cisplatin (IC₅₀ values of 7.0 μM in HT-29 cells and 2.0 μM in MCF-7 cells²⁸) and related non-metal naphthalimides (IC₅₀ values in the range of 1.9 μM to 4.6 μM²²) investigated under the same experimental conditions.

The cellular gold levels after 6 h exposure to 5 μM of **1–4** and **1a–4a** were measured by electrothermal atomic absorption spectroscopy and related to the present cell biomass (nmol Au per g cellular protein values, Fig. 3). In good agreement with the results of the proliferation experiments, the uptake of the naphthalimide

Table 1 Cell growth inhibitory effects (IC₅₀ values) and nuclear gold levels (nmol Au per g nuclear protein) of gold(i) phosphine complexes in HT-29 and MCF-7 cells

	IC ₅₀ HT-29 (μM)	IC ₅₀ MCF-7 (μM)	Nuclear Au HT-29 (nmol Au/g)	Nuclear Au MCF-7 (nmol Au/g)
1	5.2 ^{±0.6}	3.9 ^{±0.9}	21.6 ^{±0.8}	n.d.
2	5.3 ^{±1.9}	3.2 ^{±1.3}	62.4 ^{±3.0}	n.d.
3	5.2 ^{±2.1}	3.1 ^{±0.4}	84.3 ^{±25.9}	109.4 ^{±39.3}
4	4.2 ^{±0.9}	2.6 ^{±0.1}	181.8 ^{±14.2}	57.6 ^{±17.0}
1a	2.6 ^{±0.6}	1.8 ^{±0.0}	—	—
2a	2.6 ^{±0.4}	1.3 ^{±0.7}	300.3 ^{±55.1}	—
3a	2.0 ^{±0.2}	1.1 ^{±0.1}	330.8 ^{±137.8}	—
4a	3.2 ^{±1.6}	3.7 ^{±0.8}	194.2 ^{±43.4}	294.5 ^{±9.1}

n.d.: not detectable; —: no valid values obtained due to a strong reduction in cell biomass. Values for **1–4** are from ref. 25.

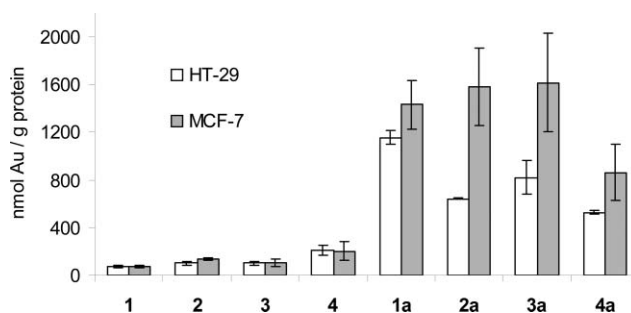


Fig. 3 Cellular uptake of 5.0 μM gold(i) phosphine complexes into HT-29 and MCF-7 cells after 6 h; in some cases the error bars are hidden behind the symbols; values of **1–4** are from ref. 25.

analogues **1a–4a** was significantly increased compared to all chloro analogues (**1–4**). This demonstrated that the organic thio-naphthalimide ligand is a useful structure to obtain complexes with enhanced cellular accumulation properties. Based on various characteristics of tumor cells the cellular molar concentrations can be estimated from the obtained cellular uptake values.²⁶ Accordingly, the values for **1a–4a** in HT-29 cells correlated to 227, 127, 162 and 104 μM, respectively. As the exposure concentration was 5.0 μM in these experiments it can be concluded that the cellular concentrations of **1a–4a** exceeded the extracellular ones at least 20 fold.

A very important observation of our previous study on **2** and **2a** was that the naphthalimide ligand caused an increased uptake of gold in the nuclei of tumor cells. Therefore, we also investigated the gold levels of nuclei isolated from cells exposed to 5.0 μM of the different gold complexes for 6 h (Table 1). Under these experimental conditions the nuclear biomass was strongly decreased (presumably to early toxic effects) for **1a–4a** making a proper analysis impossible in most cases. However, where sufficient amounts of nuclei could be obtained the respective gold levels of **1a–4a** were strongly increased compared to **1–4** confirming the previous result. Based on the elevated overall cellular uptake values of **1a–4a** it can be concluded that this strong accumulation of gold in the nuclei is also a consequence of the higher cellular gold levels caused by the presence of the naphthalimide ligand.

As this initial biological screening of **1a–4a** did not reveal substantial differences between the single complexes, we focused on **4a** in the following experiments, which is structurally most different from the previously in more detail investigated **2a**.¹⁸

Fluorescence spectroscopy and fluorescence microscopy of **4a**

Many naphthalimide compounds exhibit strong luminescence emission, which is environmentally sensitive concerning *e.g.* solvent polarity or pH.^{22,29,30} In our previous study on **2a** we reported on a decrease in fluorescence intensity upon increasing solvent polarity, which was accompanied by a red-shift and broadening of the fluorescence emission maxima.¹⁸

A 3D-scan of **4a** in DMSO showed an intensive maximum at an excitation wavelength of 438 nm (Fig. 4, top). As expected the intensity of this maximum was significantly enhanced in the apolar solvent CHCl₃ and polar media exhibited red-shifted, broadened emission maxima (emission maxima of **4a** for excitation at 438 nm: CHCl₃: 509–512 nm, DMSO: 530–538 nm, MeOH: 542–545 nm; Fig. 4, bottom). In aqueous solvents such as phosphate buffered

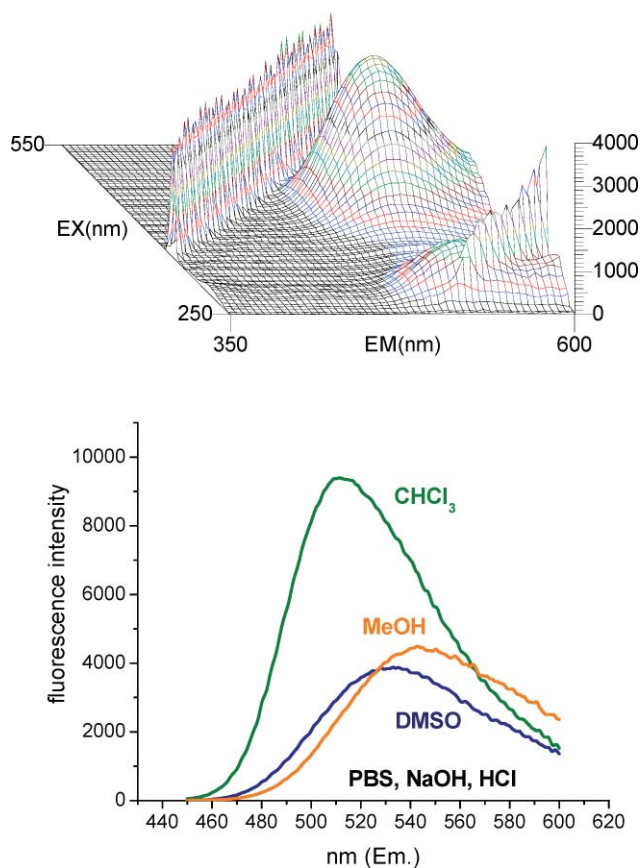


Fig. 4 Fluorescence characteristics of **4a** (5.0 μM), top: scan in DMSO, bottom: fluorescence emission scans in various solvents at an excitation wavelength of 438 nm.

saline pH 7.4 (PBS), 1 N HCl and 1 N NaOH no emission could be detected. These effects can be related to the photoinduced electron transfer (PET effect) between the side chain nitrogen and the heterocyclic naphthalimide core. PET effects can be strongly influenced by the polarity of the chemical environment.^{31,32}

With the exception of the experiments in CHCl_3 , in which **2a** had shown a maximum at Ex./Em. 440/514–518 nm,¹⁸ the emission maxima of **4a** were approximately the same as those previously reported for **2a** indicating that the influence of the substituents on the phosphine partial structure is negligible and the fluorescence characteristics of the complexes are mainly determined by the naphthalimide ligand.

The described luminescence properties enable the evaluation of cellular biodistribution by fluorescence microscopy. This method offers the opportunity to study the location of the compounds in living cells^{18,22,33,34} but has the disadvantage that it provides rather qualitative information in contrast to the quantitative information provided by other methods such as AAS^{26,35} or inductively coupled plasma mass spectrometry (ICP-MS).^{36,37} Microscopic images obtained with the compounds under study have to be interpreted with caution based on the above described fluorescence characteristics, which indicated that the complexes will be well detectable in apolar cell environments (*e.g.* membranes) but could be less visible or invisible in more polar locations such as the cytosol.

MCF-7 cells exposed to a concentration of **4a** below its IC_{50} value (2.0 μM) exhibited fluorescence emission from certain areas of the cells (top sections of Fig. 5) related to an uptake of the compound in cell organelles such as the nuclei. Exposure to a concentration of **4a** above its IC_{50} value (10 μM) led to strong fluorescence emission roughly matching to the complete cell monolayer (bottom sections of Fig. 5). At this concentration toxic effects in the cells were already relevant as observed by a detaching of cells from the well surface (Fig. 5, bottom left). In conclusion these experiments indicate that **4a** is preferentially biodistributed into the nuclei and other cell organelles and that the uptake strongly increases upon exposure to toxic concentrations, which are supposedly accompanied by a breakdown of cell membrane integrity.

Inhibition of angiogenesis in zebrafish embryos and reduction of tumor cell-induced neovascularization in a zebrafish/tumor xenograft angiogenesis assay

During our previous study on **2a** we noted a significant inhibition of angiogenesis in developing zebrafish embryos, which themselves represent a convenient model for the *in vivo* study of angiogenic processes.^{18,38,39}

Accordingly, we evaluated the inhibition of blood vessel formation in the same assay for **4a** and used **4** as a reference.

Animals exposed to **4** could not be distinguished from an untreated control (data not shown) but animals exposed to **4a** for the indicated periods exhibited relevant damages in vessel formation (as indicated by white arrows in Fig. 6) with 40–52% of the embryos being affected (see Table 2). Antiangiogenic effects can be observed in these experiments by an impaired or defective formation of intersegmental vessels (IV), dorsal longitudinal anastomic vessels (DLAV) and/or reduced subintestinal veins (SIV).

These results are in good agreement with those of our recent study on **2** and **2a**, which had given comparable results.¹⁸ As chloro gold phosphine compounds are not active in these experiments in contrast to naphthalimide gold phosphine complexes it could be concluded that the antiangiogenic effects are a consequence of the presence of the heteroaromatic ligand. In order to study this in more detail analogous experiments were performed on a non-metal naphthalimide derivative, in which the gold phosphine partial structure was replaced by an ethyl group, and indeed similar results were observed (see ESI for details†).

Recently, a novel *in vivo* tumor xenograft angiogenesis assay (neovascularization assay) has been established in zebrafish

Table 2 Inhibition of angiogenesis in developing zebrafish embryos

	24 h	48 h	72 h	96 h
	% defects	% defects	% defects	% defects/% alive
Control	0	0	0	0/91 ^{±7}
4 0.01 μM	0	0	0	0/90 ^{±3}
4 0.05 μM	0	0	0	0/89 ^{±2}
4a 0.01 μM	40 ^{±9}	52 ^{±2}	52 ^{±1}	51 ^{±1} /96 ^{±5}
4a 0.05 μM	42 ^{±3}	49 ^{±3}	50 ^{±2}	49 ^{±2} /90 ^{±6}

Given are the percentages of embryos with defects in DLAV or/and SIV formation after the indicated period and the percentages of embryos alive after 96 h.

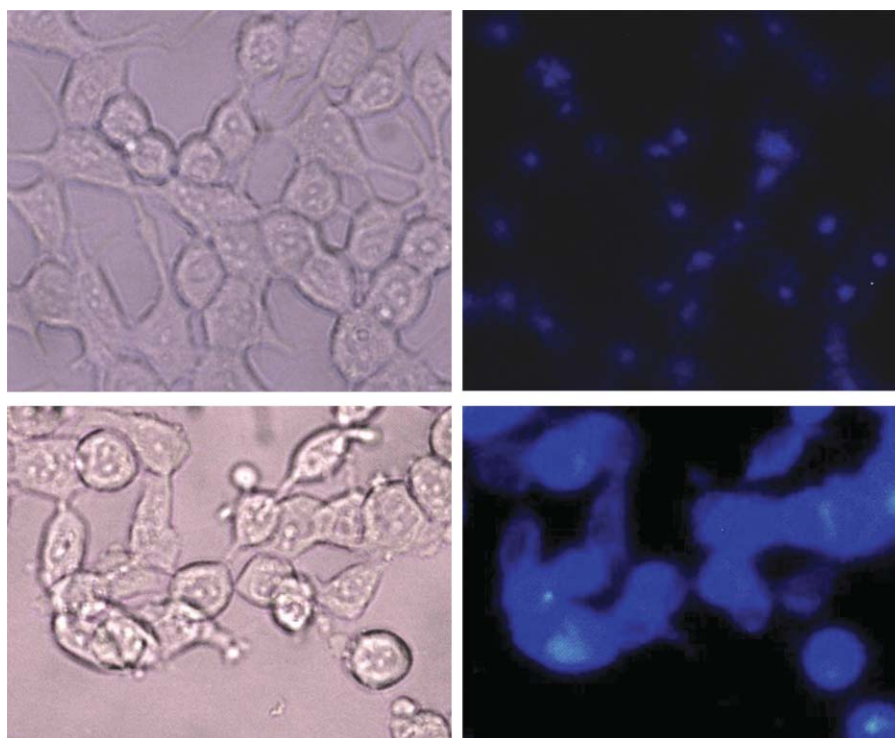


Fig. 5 Microscopic pictures of MCF-7 cells exposed to **4a** for 6 h; top left: 2.0 μM **4a**, brightfield image, top right: 2.0 μM **4a**, fluorescence image; bottom left: 10 μM **4a**, brightfield image; bottom right: 10 μM **4a**, fluorescence image.

Table 3 Inhibition of tumor-cell induced neovascularization in developing zebrafish embryos transplanted with human pancreatic cancer cells

	4 (% positive)	4a (% positive)
0 μM (solvent control)	84 ^{±4}	84 ^{±4}
0.05 μM	70 ^{±2}	19 ^{±2}
0.1 μM	77 ^{±2}	14 ^{±4}

Given are the percentages of embryos with induced vessel formation at 24 h post injection of tumor cells. Three independent experiments were performed and for each concentration and compound 100 embryos were investigated. The assay was essentially performed as previously described.⁴¹ Non-transplanted zebrafish embryos do not show a similar formation of microvasculature from the SIV (data not shown).

embryos.^{40,41} This novel model system allows us to follow the induction of blood vessel formation by xenotransplanted proangiogenic human cancer cells in real-time in living zebrafish and enables the quantification of neovascularization *in vivo* and in high-resolution. In this study we used this tumor-cell induced angiogenesis model in order to investigate the effects of **4** and **4a** on the induction of new blood vessels by transplanted human pancreatic tumour cells (PaTu-8998T cells).^{42,43} Our results show inhibitory effects of **4a** on tumor-cell induced angiogenesis. **4a** at two non-lethal concentrations strongly inhibited the induction of new microvasculature in the zebrafish neovascularization assay when added to the water containing the zebrafish embryos (Fig. 7 and Table 3). A final concentration of 0.1 μM of compound **4a** led to an 83% reduction of tumor-induced angiogenesis when compared to the solvent control DMSO (Table 3). In contrast, compound **4** at the same final concentration of 0.1 μM showed minor effects and led only to 9% reduction of tumor-induced neovascularization,

when normalized to the solvent control (Table 3). Comparative studies with the non-metal naphthalimide derivative mentioned above again revealed comparable effects (see ESI†).

Taken together, these data show that compound **4a** has antiangiogenic properties and inhibits both, angiogenesis in developing zebrafish embryos as well as tumor-cell induced angiogenesis. These effects could be clearly related to the presence of the organic naphthalimide ligand.

Conclusion

A series of thio-naphthalimide gold(i) phosphine complexes (**1a–4a**) displayed promising cell growth inhibiting potencies. Atomic absorption spectroscopy studies showed a stronger uptake into the tumor cells as well as an enhanced accumulation of gold in the nuclei of the cells for **1a–4a** compared to the respective chloro analogues **1–4**. However, comparing the results obtained with **1a–4a** it is obvious that the nature of the alkyl/aryl substituents on the phosphor did not have a strong impact on bioactivity.

The triphenylphosphine analogue **4a** was selected for more detailed studies. Fluorescence spectroscopic and fluorescence microscopic experiments indicated a significant influence of the solvent polarity on the emission intensities and an uptake into cell compartments including the nuclei. Additionally, **4a** exhibited strong antiangiogenic effects in developing zebrafish embryos concerning “normal” angiogenesis and tumor-induced angiogenesis. As the chloro analogue **4** was not active in this assay and a non-metal naphthalimide derivative triggered similar effects, it can be concluded that the antiangiogenic effects are a consequence of the presence of the thio-naphthalimide ligand.

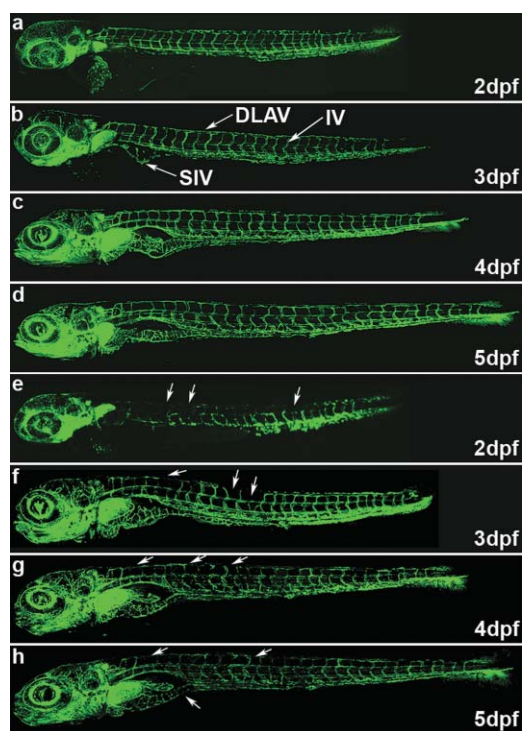


Fig. 6 Angiogenesis assay. Tg:flil-1/EGFP embryos were either treated with compound **4** (a–d) or **4a** (e–h). Pictures shown are examples of embryos from 2 to 5 days post fertilization (dpf). The compounds were added to the water containing 1 dpf dechorionated embryos at a final concentration of 0.05 μM . In image b, an intersegmental vessel (IV), a dorsal longitudinal anastomotic vessel (DLAV) and the subintestinal vein (SIV) are indicated by arrows. Arrows in e–h point to vessel defects in the embryos treated with compound **4a**. All fluorescence images of the Tg:flil1/eGFP zebrafish were taken by laser scanning confocal microscopy.

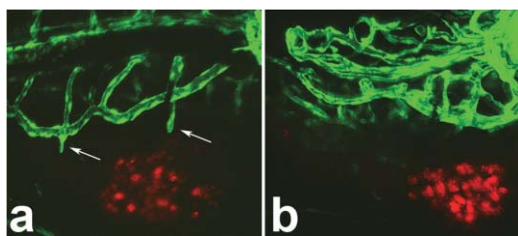


Fig. 7 Tumor-induced angiogenesis. Shown are example pictures obtained with the recently described neovascularization assay.⁴¹ Human pancreatic tumor cells (PaTu-8998T cells) were transplanted close to the developing subintestinal vein (SIV) into 48 hpf Tg:flil-1/EGFP embryos. Immediately after transplantation, zebrafish embryos were either treated with **4** (left image) or **4a** (right image) and 24 h later investigated for the formation of new vasculature from the SIV. Compound **4a** showed strong inhibition of tumor-induced angiogenesis, whereas **4** had a minor effect both compared to the solvent control (see Table 3).

As the mode of molecular target interaction of gold phosphine thiolate complexes is based on a loss of coordinated ligands and the agents are therefore not completely stable during *in vitro*/*in vivo* experiments, the nature of the active species of the studied compounds (or related complexes already used as antirheumatic drugs, respectively) is not completely clear at this stage.⁴⁴ For example, for auranofin it was reported that its thiolate ligand was lost during cell culture experiments. Furthermore, this drug

supposedly interacts with TrxR by covalent binding, which in turn requires the removal of a coordinated ligand.^{8,19,20} For the complexes described here it was observed that exposure of cells to the naphthalimide containing derivatives **1a–4a** yielded elevated gold levels in the cells and in nuclei isolated from the cells. This suggests on the one hand that the organic ligand transports gold into the cells and nuclei and on the other hand that the gold–sulfur bond can be considered to be sufficiently stable under *in vitro* conditions (although it is very likely that the complexes react with biomolecules over time and different gold species are formed continuously). In this context it also should be noted that previous studies on the interaction between **2a** and a cysteine containing model peptide had indicated that the phosphine ligand is more stably bound to the gold central atom than the thiolate ligand.¹⁸

Further studies on the evaluation of the biological profile of these and structurally related gold metallodrugs are ongoing.

Experimental

General

Chemicals and reagents were purchased from Sigma, Aldrich or Fluka. **2a** and 4-mercapto-1,8-naphthalic anhydride were prepared as previously described.¹⁸ PBS: phosphate buffered saline pH 7.4; NMR spectra were recorded on a 400 MHz spectrometer (Avance/DPX 400, Bruker); elemental analysis: Perkin-Elmer 240 C; MS spectra: CH-/A-Varian MAT (70eV).

Synthesis; general procedure

An amount of 100–120 mg 4-mercapto-1,8-naphthalic anhydride was suspended in 15 mL of absolute ethanol, and 0.25 mL (2.29 mmol) 2-(dimethylamino)ethylamine were added. The resulting mixture was slowly heated and finally kept under reflux heating for 6 h. The solvent was removed by evaporation, and the remaining dark red oil was dried. The residue was dissolved in 10 mL of absolute CH_2Cl_2 , and 100–110 mg of **1**, **3** or **4** and 0.2 g (1.45 mmol) of anhydrous K_2CO_3 were added. The resulting mixture was stirred at room temperature for 5 h. The solvent was evaporated and the product isolated by column chromatography (stationary phase: silica, mobile phase: CH_2Cl_2 followed by $\text{CH}_2\text{Cl}_2/\text{MeOH}$ 9/1).

[N-(N',N'-Dimethylaminoethyl)-1,8-naphthalimide-4-sulfide](trimethyl-phosphine)gold(I) (**1a**)

116 mg (0.50 mmol) 4-mercapto-1,8-naphthalic anhydride; 103 mg (0.33 mmol) **1**, yield: 77 mg, red-orange crystals (0.13 mmol, 39%); ¹H-NMR (CDCl_3): (ppm) 1.66 (d, 9H, -P- CH_3), 2.37 (s, 6H, -N(CH_3)₂), 2.66 (t, 2H, ³J = 7.2 Hz, CH_2), 4.31 (t, 2H, ³J = 7.2 Hz, CH_2), 7.67 (dd, 1H, ³J = 7.3 Hz, 1H, ³J = 8.4 Hz, ArH6), 8.14 (d, 1H, ³J = 7.8 Hz, ArH3), 8.26 (d, 1H, ³J = 7.8 Hz, ArH2), 8.57 (dd, 1H, ³J = 7.3 Hz, ⁴J = 0.9 Hz ArH5), 9.04 (dd, 1H, ³J = 8.4 Hz, ⁴J = 0.9 Hz ArH7); MS (EI): m/z: 573.1 (M + H⁺); elemental analyses (calc./found): C (39.87/40.04), H (4.23/4.42), N (4.89/5.10).

(tri-*tert*-Butylphosphine)[*N*-(*N,N'*-dimethylaminoethyl)-1,8-naphthalimide-4-sulfide]gold(I) (**3a**)

103 mg (0.45 mmol) 4-mercapto-1,8-naphthalic anhydride; 108 mg (0.25 mmol) **3**, yield: 80 mg, red-orange crystals (0.11 mmol, 44%); ¹H-NMR (CDCl₃): (ppm) 1.56 (m, 27H, -C(CH₃)₃), 2.37 (s, 6H, -N(CH₃)₂), 2.66 (t, 2H, ³J = 7.2 Hz, CH₂), 4.31 (t, 2H, ³J = 7.2 Hz, CH₂), 7.66 (dd, 1H, ³J = 8.5 Hz, ³J = 7.3 Hz, ArH6), 8.19 (d, 1H, ³J = 7.9 Hz, ArH3), 8.24 (d, 1H, ³J = 7.9 Hz, ArH2), 8.56 (dd, 1H, ³J = 7.3 Hz, ⁴J = 1.2 Hz, ArH5), 9.08 (dd, 1H, ³J = 8.5 Hz, ⁴J = 1.2 Hz, ArH7); MS (EI): *m/z*: 699.2 (M + H⁺); elemental analyses (calc./found): C (48.18/48.15), H (6.06/6.22), N (4.01/3.90).

[*N*-(*N,N'*-Dimethylaminoethyl)-1,8-naphthalimide-4-sulfide](triphenyl-phosphine)gold(I) (**4a**)

105 mg (0.46 mmol) 4-mercapto-1,8-naphthalic anhydride; 112 mg (0.23 mmol) **4**, yield: 96 mg, red-orange crystals (0.13 mmol, 56%); ¹H-NMR (CDCl₃): (ppm) 2.36 (s, 6H, -N(CH₃)₂), 2.65 (t, 2H, ³J = 7.2 Hz, CH₂), 4.31 (t, 2H, ³J = 7.2 Hz, CH₂), 7.45–7.57 (m, 14H, ArH), 7.65–7.70 (m, 2H, ArH), 8.25 (m, 2H, ArH2, ArH3), 8.58 (m, 1H, ArH5), 9.10 (m, 1H, ArH7); MS (EI): *m/z*: 759.2 (M + H⁺); elemental analyses (calc./found): C (53.83/53.92), H (3.99/4.06), N (3.69/3.63).

Antiproliferative effects

The antiproliferative effects in MCF-7 and HT-29 cells after 72 h (HT-29) or 96 h (MCF-7) exposure to the gold complexes were evaluated according to recently described procedures.^{22,27} For the experiments the compounds were prepared freshly as stock solutions in DMF and diluted with the cell culture medium to the final assay concentrations (0.1% V/V DMF). The IC₅₀ value was described as that concentration reducing proliferation of untreated control cells by 50%.

Uptake of gold into the cells and into the nuclei

Cells were grown until at least 70% confluency in 75 cm² cell culture flasks. The compounds were prepared freshly as stock solutions in DMF and diluted with the cell culture medium to a concentration of 5.0 μM (0.1% V/V DMF). The cell culture medium was removed and replaced with fresh medium containing the gold complexes. After 6 h exposure, the gold content of isolated cells and isolated cell nuclei were measured by graphite furnace atomic absorption spectroscopy and measured gold levels were related to the protein contents of the cells and nuclei as described in more detail recently.^{18,25,26}

Fluorescence spectroscopy

All solvents used for the fluorimetric experiments were purged with nitrogen prior to use. **4a** was dissolved as a stock solution (500 μM) in DMF, diluted 100 fold with the respective solvents (CHCl₃, DMF, DMSO, MeOH, PBS, 1 N NaOH and 1 N HCl) and measured using a Hitachi F-4500 fluorescence spectrometer. Only corrected spectra were taken.

Fluorescence microscopy of tumor cells

Cells were grown in 6-well plates (Sarstedt) until at least 70% confluency. The compounds were prepared freshly as stock solutions in DMF and diluted with the cell culture medium to the final assay concentrations (2.0 μM and 10 μM, 0.1% V/V DMF). The cell culture medium was replaced with fresh medium containing **4a** and incubated for 6 h at 37 °C in a 5% CO₂/95% air atmosphere. The medium was removed, the cells were washed with PBS and finally 500 μL PBS was added to each well. Microscopy was performed using a Axiovert 40 CFL microscope (Zeiss) equipped with a 50 W mercury vapor short arc lamp and a Ex/Em 390¹¹/460²⁵ nm filter.

Animal care and handling

Transgenic zebrafish (*Danio rerio*) Tg(fli1:eGFP) were handled in compliance with local animal care regulations and standard protocols of the Netherlands. Fish were maintained at 28 °C in aquaria with day/night light cycles (10 h dark *versus* 14 h light periods). The fish were crossed in the afternoon and eggs were harvested the next morning.

Live imaging of angiogenesis

Substances were administered once to dechorionated (24 h post fertilization) hpf embryos. For this purpose, complexes were dissolved in DMF and the stock solutions were diluted (1 : 1000) with the water containing the embryos to the final concentrations of 0.01 and 0.05 μM. The control solutions contained the same concentration of DMF (0.1%). The Biorad Confocal microscope 1024ES (Zeiss microscope) was used for investigating vessel defects in the tranquilized (0.042 mg/mL tricaine (Sigma, St. Luis, MO)) Tg(fli1:eGFP) fish.

Cell culture and staining of human pancreatic cancer cells^{42,43}

PaTu8988T cells were cultured in DMEM high glucose, with 10% FCS and 1 : 100 Pen/Strep. After trypsinization, cells were twice washed with 67% DPBS (GIBCO, Invitrogen), transferred to 1.5 mL Eppendorf tubes and centrifuged for 5 min at 1500 rpm. Cells were resuspended in 250 μL staining solution (67% DPBS containing 4 ng/μL final concentration of CellTracker CM-Dil (Invitrogen, Eugene, Oregon, USA). Cells were incubated at 37 °C for 4 min followed by a 15 min incubation period at 4 °C. After an initial washing step in 1.0 mL 100% FCS (Sigma) the cells were twice washed with 67% DBPS.

Tumor-cell induced angiogenesis^{40,41}

48 hpf zebrafish embryos were dechorionated and anesthetized using 0.042 mg/mL Tricaine (Sigma, St. Luis, MO) and put on a 1.8% agarose dish for injections. Cells were prepared as described above, then suspended in 20 μL 12.0 mg/mL Matrigel solution (Cultrex R Basement Membrane Extract, R and D systems, Minneapolis, USA) and kept on ice for a short period of time until injection. The CellTram Oil injector (Eppendorf, Hamburg, Germany) was loaded by using a manual injector (Eppendorf; Injectman NI2). An aliquot of 5 μL of the cell suspension in Matrigel was loaded into an injection needle, and embryos were injected as described in more detail in the

literature.^{40,41} Complexes were dissolved in DMF and the stock solutions were diluted (1:1000) with the water containing the embryos to the final concentrations of 0.01 and 0.05 μM . The control solutions contained the same concentration of DMF (0.1%). After injection, embryos were incubated at 35 °C for 24 h. Afterwards, embryos were checked and photographed using the Biorad confocal microscope 1024ES (Zeiss microscope).

Acknowledgements

Financial support by DFG (Deutsche Forschungsgemeinschaft) and GIF (German–Israeli Foundation) is gratefully acknowledged. I. O. wants to thank Prof. R. Gust from Freie Universität Berlin for generous access to all facilities of his laboratories.

References

- 1 M. Galanski, M. A. Jakupec and B. K. Keppler, *Curr. Med. Chem.*, 2005, **12**, 2075.
- 2 I. Ott and R. Gust, *Anti-Cancer Agents Med. Chem.*, 2007, **7**, 95.
- 3 E. Meggers, *Curr. Opin. Chem. Biol.*, 2007, **11**, 287.
- 4 P. C. A. Bruijninx and P. J. Sadler, *Curr. Opin. Chem. Biol.*, 2008, **12**, 197.
- 5 M. A. Jakupec, M. Galanski, V. B. Arion, C. G. Hartinger and B. K. Keppler, *Dalton Trans.*, 2008, 183.
- 6 I. Ott and R. Gust, *Arch. Pharm.*, 2007, **340**, 117.
- 7 U. Schatzschneider and N. Metzler-Nolte, *Angew. Chem., Int. Ed.*, 2006, **45**, 1504.
- 8 I. Ott, *Coord. Chem. Rev.*, 2009, **253**, 1670.
- 9 A. Bindoli, M. P. Rigobello, G. Scutari, C. Gabbiani, A. Casini and L. Messori, *Coord. Chem. Rev.*, 2009, **253**, 1692.
- 10 P. J. Barnard and S. J. Berners-Price, *Coord. Chem. Rev.*, 2007, **251**, 1889.
- 11 J. L. Hickey, R. A. Ruhayel, P. J. Barnard, M. V. Baker, S. J. Berners-Price and A. Filipovska, *J. Am. Chem. Soc.*, 2008, **130**, 12570.
- 12 M. M. Jellicoe, S. J. Nichols, P. A. Callus, M. V. Baker, P. J. Barnard, S. J. Berners-Price, J. Whelan, G. C. Yeoh and A. Filipovska, *Carcinogenesis*, 2008, **29**, 1124.
- 13 A. Casini, M. A. Cinellu, G. Minghetti, C. Gabbiani, M. Coronello, E. Mini and L. Messori, *J. Med. Chem.*, 2006, **49**, 5524.
- 14 R. W. Y. Sun, D. L. Ma, E. L. M. Wong and C. M. Che, *Dalton Trans.*, 2007, 4884.
- 15 V. Milacic and Q. P. Dou, *Coord. Chem. Rev.*, 2009, **253**, 1649.
- 16 R. W. Y. Sun and C. M. Che, *Coord. Chem. Rev.*, 2009, **253**, 1682.
- 17 Y. Wang, Q. Y. He, C. M. Che, S. W. Tsao, R. W. Sun and J. F. Chiu, *Biochem. Pharmacol.*, 2008, **75**, 1282.
- 18 I. Ott, X. Qian, Y. Xu, D. H. W. Vlecken, I. J. Marques, D. Kubuat, J. Will, W. S. Sheldrick, P. Jesse, A. Prokop and C. P. Bagowski, *J. Med. Chem.*, 2009, **52**, 763.
- 19 R. M. Snyder, C. K. Mirabelli and S. T. Crooke, *Biochem. Pharmacol.*, 1986, **35**, 923.
- 20 R. M. Snyder, C. K. Mirabelli and S. T. Crooke, *Biochem. Pharmacol.*, 1987, **36**, 647.
- 21 M. F. Brana and A. Ramos, *Curr. Med. Chem.: Anti-Cancer Agents*, 2001, **1**, 237.
- 22 I. Ott, Y. Xu, J. Liu, M. Kokoschka, M. Harlos, W. S. Sheldrick and X. Qian, *Bioorg. Med. Chem.*, 2008, **16**, 7107.
- 23 H. Zhu, M. Huang, F. Yang, Y. Chen, Z. H. Miao, X. H. Qian, Y. F. Xu, Y. X. Qin, H. B. Luo, X. Shen, M. Y. Geng, Y. J. Cai and J. Ding, *Mol. Cancer Ther.*, 2007, **6**, 484.
- 24 A. Wu, Y. Xu and X. Qian, *Bioorg. Med. Chem.*, 2009, **17**, 592.
- 25 H. Scheffler, Y. Ya and I. Ott, *Polyhedron*, 2009, DOI: 10.1016/j.poly.2009.06.007.
- 26 I. Ott, H. Scheffler and R. Gust, *ChemMedChem*, 2007, **2**, 702.
- 27 I. Ott, T. Koch, H. Shorafa, Z. Bai, D. Poeckel, D. Steinhilber and R. Gust, *Org. Biomol. Chem.*, 2005, **3**, 2282.
- 28 S. Schäfer, I. Ott, R. Gust and W. S. Sheldrick, *Eur. J. Inorg. Chem.*, 2007, 3034.
- 29 J. Huang, Y. Xu and X. Qian, *Org. Biomol. Chem.*, 2009, **7**, 1299.
- 30 Z. Xu, X. Qian and J. Cui, *Org. Lett.*, 2005, **7**, 3029.
- 31 B. Ramachandram, G. Saroja, N. B. Sankaran and A. Samanta, *J. Phys. Chem. B.*, 2000, **104**, 11824.
- 32 B. Ramachandram, *J. Fluoresc.*, 2005, **15**, 71.
- 33 E. J. New, R. Duan, J. Z. Zhang and T. W. Hambley, *Dalton Trans.*, 2009, 3092.
- 34 F. Noor, R. Kinscherf, G. A. Bonaterra, S. Walczak, S. Wölfl and N. Metzler-Nolte, *ChemBioChem*, 2009, **10**, 493.
- 35 S. I. Kirin, I. Ott, R. Gust, W. Mier, T. Weyhermüller and N. Metzler-Nolte, *Angew. Chem., Int. Ed.*, 2008, **47**, 955.
- 36 E. Gabano, E. Colangelo, A. R. Ghezzi and D. Osella, *J. Inorg. Biochem.*, 2008, **102**, 629.
- 37 M. Groessl, C. G. Hartinger, P. J. Dyson and B. K. Keppler, *J. Inorg. Biochem.*, 2008, **102**, 1060.
- 38 I. Ott, B. Kircher, C. P. Bagowski, D. H. W. Vlecken, E. B. Ott, J. Will, K. Bendorf, W. S. Sheldrick and R. Gust, *Angew. Chem., Int. Ed.*, 2009, **48**, 1160.
- 39 N. D. Lawson and B. M. Weinstein, *Dev. Biol.*, 2002, **248**, 307.
- 40 S. Nicoli and M. Presta, *Nat. Protoc.*, 2007, **2**, 2918.
- 41 S. Nicoli, D. Ribatti, F. Cotelli and M. Presta, *Cancer Res.*, 2007, **67**, 2927.
- 42 H. P. L. U. Elsässer, B. Agricola and H. F. Kern, *Virchows Archiv B Cell Pathology Including Molecular Pathology*, 1992, **61**, 295.
- 43 I. J. Marques, F. U. Weiss, D. H. Vlecken, C. Nitsche, J. Bakkers, A. K. Lagendijk, L. I. Partecke, C. D. Heidecke, M. M. Lerch and C. P. Bagowski, *BMC Cancer*, 2009, **9**, 128.
- 44 C. F. Shaw, *Chem. Rev.*, 1999, **99**, 2589.